Chemical Engineering Division, ASEE
1999 Union Carbide Award Lecture

PARTICLE DYNAMICS IN FLUIDIZATION AND FLUID-PARTICLE SYSTEMS

*Part 2. Teaching Examples**

LIANG-SHIH FAN
The Ohio State University • Columbus, OH 43210

In Part 1 of this lecture, I discussed the general educational issues concerning particle technology, with specific emphasis on fluidization and fluid-particle systems. In this part I will discuss some pertinent materials pertaining to fluidization and fluid-particle systems that could readily be integrated into existing required chemical engineering course materials. These materials, each introduced to students for a specific purpose, cover both gas-solid and gas-liquid-solid fluidization systems. In addition, I will discuss relevant commercial codes that are available for students to learn about the computation of fluid-particle systems. Some representative results marking the state-of-the-art efforts in computational fluid dynamics of fluidization will also be given.

L.-S. Fan is Distinguished University Professor and Chairman of the Department of Chemical Engineering at The Ohio State University. His expertise is in fluidization and multiphase flow, powder technology, and particulates reaction engineering. Professor Fan is the U.S. editor of *Powder Technology* and a consulting editor of the *AIChE Journal* and the *International Journal of Multiphase Flow*. He has authored or co-authored three books, including *Principles of Gas-Solid Flows* (with Chao Zhu; Cambridge University Press, 1998).

Professor Fan is the principal inventor (with R. Agnihotri) of a patented process, "OSCAR," for flue gas cleaning in coal combustion and is the Project Director for the OSCAR commercial demonstration, funded at $8.5 million as Ohio Clean Coal Technology, currently taking place at Ohio McCracken power plant on The Ohio State University campus.

He has served as thesis advisor for two BS, twenty-nine MS, and forty-two PhD students at Ohio State, and is a Fellow of the American Association for the Advancement of Science and the AIChE.

* *Part 1 of this Award Lecture appeared in the Winter '00 issue of* Chemical Engineering Education *(CEE, **34**(1), p. 40, 2000).*

SAMPLE SUBJECTS OF PERTINENCE TO CHEMICAL ENGINEERS

It is ideal to encompass both the two-phase and three-phase systems in the teaching of fluidization as these two systems behave significantly differently. Salient subjects concerning gas-solid fluidization and gas-liquid-solid fluidization are given below.

Flow surrounding a bubble, two-phase theory, and flow segregation • *introduced so students will be familiar with the use of proper assumptions for developing theories that capture the dominant behavior features.*

Gas-solid fluidization phenomena are strongly dependent on the physical properties of the solid particles employed. Therefore, it would be appropriate to introduce the classification of fluidized particles to the student. Particles are classified into four groups (*i.e.,* Groups A, B, C, and D) based on their fluidization behavior. This classification, known as Geldart's classification,[1] is shown in Figure 1, where particles are classified in terms of the density difference between the particles and the gas, $(\rho_p - \rho)$, and the average particle diameter, d_p. Figure 1 was obtained empirically and has been widely adopted in the fundamental research and design of gas-solid fluidized beds. Group C comprises small cohesive particles ($d_p < 20$ μm). Group A particles, with a typical size range of 30 to 100 μm, are readily fluidized. For Group B particle fluidization, there exists no maximum stable bubble size. Group D comprises coarse particles ($d_p > 1$ mm), which are commonly

processed by spouting.

We would then demonstrate to the student the rise of a bubble or slug in a dense gas-solid suspension using a simple known experiment that involves placing fine particles (FCC, Group A particles) in a sealed tube. The tube is 58 cm long and 87% full of particles. As shown in Figure 2, when the tube is flipped upside down a slug rises in the tube (Figure 2a). When the slug exits to the top of the tube, it leaves behind a dense particle bed (Figure 2b) that has a height higher than the packed condition of the particles (Figure 2c). The physical implication from comparing Figures 2b and 2c is that a bed of fine particles can be expanded by gas to an extended height without the formation of bubbles. This would lead to a discussion of the onset of bubbling.

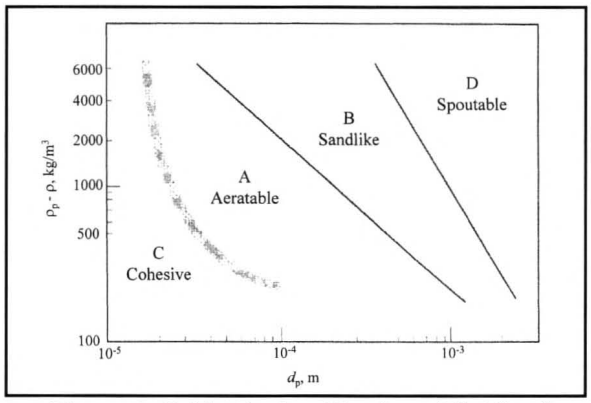

Figure 1. *Geldart's classification of fluidized particles.*[1]

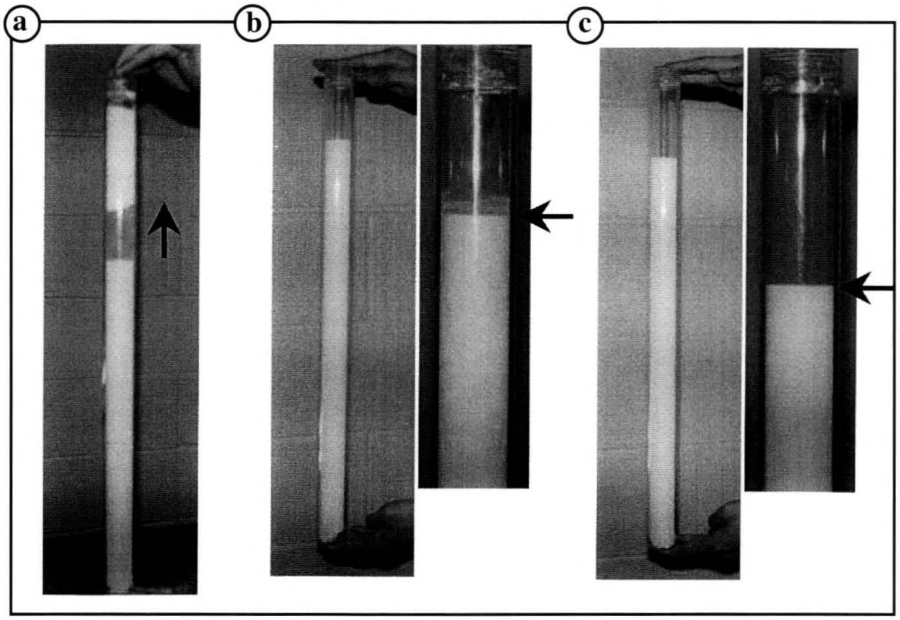

Figure 2. *Simple fluidization experiments: (a) slugging regime, (b) particulate fluidization regime, and (c) packed-bed regime.*

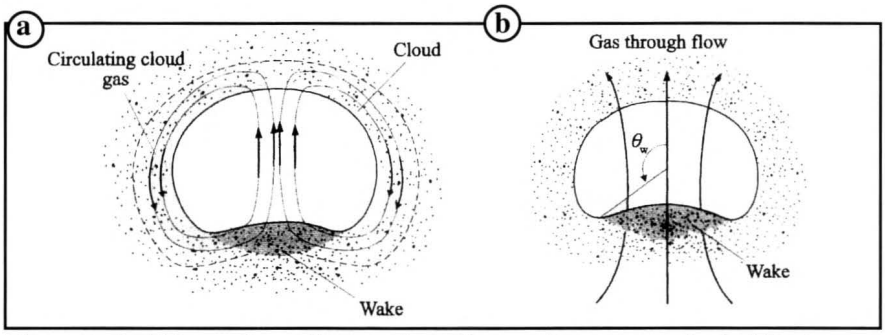

Figure 3. *Bubble configurations and gas-flow patterns around a bubble in gas-solid fluidized beds. (a) Fast bubble (clouded bubble)* $U_b > U_{mf} / \alpha_{mf}$ *; (b) Slow bubble (cloudless bubble)* $U_b < U_{mf} / \alpha_{mf}$.

Bubbles are formed as a result of the inherent instability of gas-solid systems. The instability of a gas-solid fluidized bed is characterized by fast growth in local voidage in response to a system perturbation. Because of the instability in the bed, the local voidage usually grows rapidly into a shape resembling a bubble. Although it is not always true, the initiation of the instability is usually perceived as the onset of bubbling, which marks the transition from particulate fluidization to bubbling fluidization. The theoretical explanation of the physical origin and prediction of the onset of the instability of gas-solid fluidized beds has been attempted.[2] Efforts have focused on the primary forces behind the stability among interparticle contact forces, particle-fluid interaction forces, and particle-particle interaction via particle velocity fluctuation.

Fluidization of fine particles (Group A particles) without the formation of bubbles is known to be in the particulate fluidization regime. For large and/or heavy particles (*i.e.,* Group B or D particles), particulate fluidization does not exist. That is, the onset of bubbling coincides with that of minimum fluidization of the packed bed.

Most bubbles in gas-solid fluidized beds are of spherical cap or ellipsoidal cap shape. Configurations of two basic types of bubbles, fast bubble (clouded bubble) and slow bubble (cloudless bubble)[3] are schematically depicted in Figure 3. The cloud is the region established by the gas that circulates in a closed loop between the bubble and its surroundings. The cloud phase can be visualized with the aid of a color tracer gas bubble. For example, when a dark brown NO_2 bubble is injected into the bed (see Figure 4), the light brown color surrounding the bubble represents the cloud region.[4] When the bubble-rise velocity is higher than the interstitial-gas velocity, a "clouded" bubble forms in which the circulatory flow of gas takes place between the bubble and the cloud, as shown in Figure 3a. The cloud size decreases as the bubble-rise velocity increases. As the

bubble-rise velocity becomes significantly higher than the interstitial-gas velocity (*i.e.*, U_{mf} / α_{mf}), the cloud size becomes so thin that most of the gas circulates inside the bubble. When the interstitial-gas velocity is greater than the bubble-rise velocity, it yields a "cloudless" bubble in which the emulsion phase gas flows through the bubble phase, as shown in Figure 3b. This gas through-flow in the bubble is also known as invisible bubble flow, which is distinguishable from visible bubble flow. Bubbles in Group D particle fluidized beds are typically characterized by cloudless bubbles.

To describe the complex particle and gas flows around the bubble in the fluidized beds described above, we introduce the model of Davidson and Harrison[5] because of its fundamental importance and relative simplicity. The model employs the following key assumptions:

1. *The bubble is solids-free and spherical, and has a constant internal pressure.*
2. *The emulsion phase is a pseudocontinuum, an incompressible and inviscid single fluid with an apparent density of* $\rho_p(1-\alpha_{mf})+\rho\alpha_{mf}$.

With these assumptions, the velocity and pressure distributions of the "fluid" in a uniform potential flow field around a bubble, as portrayed in Figure 5, can be given as[5]

$$U_{pf} = -U_{b\infty}\left(1-\frac{R_b^3}{r^3}\right)\cos\theta$$

$$V_{pf} = U_{b\infty}\left(1+\frac{R_b^3}{2r^3}\right)\sin\theta \qquad (1)$$

and

$$p_{pf} = p_{pf}\Big|_{z=0} + \left(\frac{\partial p_{pf}}{\partial z}\right)_{\infty}\left(r-\frac{R_b^3}{r^2}\right)\cos\theta \qquad (2)$$

where the subscripts "pf" and "∞" represent the pseudofluid and the undisturbed conditions, respectively, $U_{b\infty}$ is the rise velocity of an isolated bubble, and R_b is the bubble radius. The pressure far away from the rising bubble in a fluidized bed can be approximated at minimum fluidization. Thus, Eq. (2) becomes

$$p_{pf} = p_{pf}\Big|_{z=0} - (\rho_p-\rho)(1-\alpha_{mf})g\left(r-\frac{R_b^3}{r^2}\right)\cos\theta \qquad (3)$$

Figure 6 shows a good comparison between the measured dynamic pressure and the calculated results based on Eq. (3). The profile indicates that there is a local high-pressure region near the bubble nose and a local low-pressure region around the bubble base, *i.e.*, the wake region. The low pressure in the wake region promotes pressure-induced bubble coalescence in the bed.

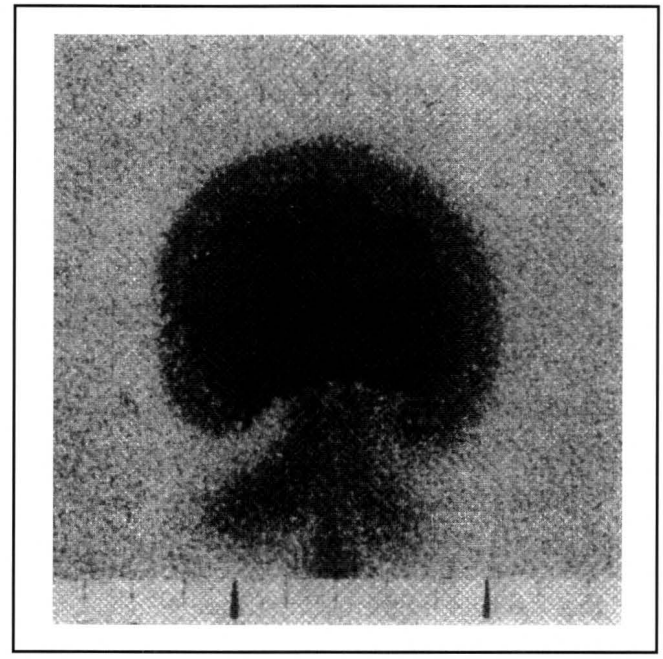

Figure 4. *An NO_2 bubble rising in a two-dimensional ballotini bed showing the cloud region of the bubble (from Rowe;[4] reproduced with permission).*

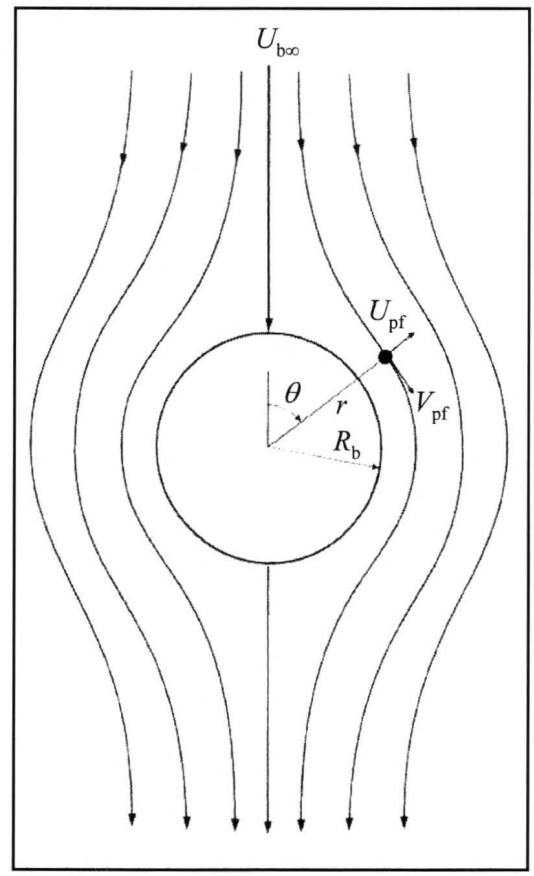

Figure 5. *Potential flow around a spherical bubble in a two-dimensional projection (from Davidson and Harrison[5]).*

The macroscopic behavior of a fluidized bed can be described using the two-phase theory of fluidization.[9] This theory considers the bed to be divided into two phases, *i.e.,* the bubble phase and the emulsion phase, as shown in Figure 7, with a corresponding division of superficial gas flow in the bed to each of the two phases, *i.e.,* U_{em} to the emulsion phase and $\alpha_b U_{bb}$ to the bubble phase, where α_b is the volume fraction of bubbles in the bed, and U_{bb} is the average bubble-rise velocity in the bed. Many analyses of transport phenomena of a bubbling fluidized bed are made based on this simple two-phase theory. The two-phase theory concept is also extended to describe the macroscopic flow behavior of high-velocity fluidization in which the core-annular flow structure prevails in the column. In fluidization, particle collisions and particle-turbulence interaction yield a dense, wavy, clustering solids layer in the wall region and dilute solids in the core region. The core region and wall region can be treated as two interpenetrating phases in the analysis of this flow behavior.

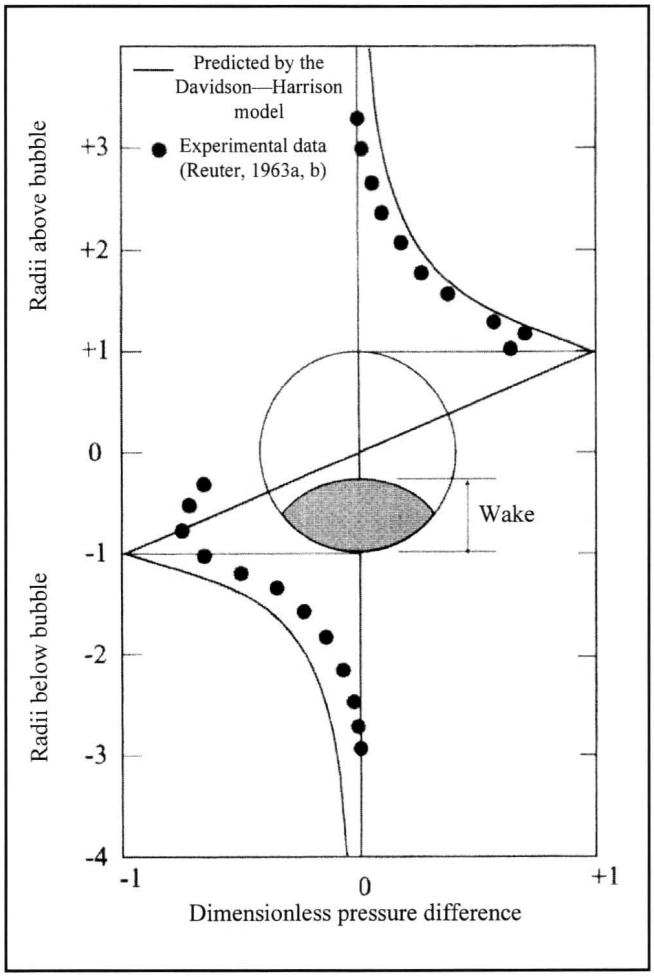

Figure 6. *Pressure distribution in the vicinity of a rising three-dimensional bubble with a comparison of the experimental data by Reuter[6,7] and the Davidson-Harrison model prediction (from Stewart[8]).*

Phenomena of bubble wake dynamics in liquid-solid suspensions • *introduced so students will understand the importance of identification of the governing factors underlying complex phenomena*

A large number of liquid-solid fluidized beds are operated in the presence of gas bubbles. In both reactive and non-reactive systems, gas bubbles play an essential role in determining the behavior or performance of the bed. For example, gas bubbles are usually a source of reactant gas species whose transport phenomena often depend on the fluid flow around the bubble; gas bubbles induce intimate liquid/solids mixing; and in a three-phase fluidized bed, gas bubbles are responsible for solids entrainment to the freeboard and bed contraction. It has been specifically recognized that the bubble wake located immediately underneath the bubble base is the dominating factor contributing to bed performance. It is, thus, of primary importance for students to understand the fluid dynamic behavior of the bubble wake and its interaction with the bubbles so that they will be vested with sound, fundamental knowledge in their efforts toward modeling, simulation, and design of such particulate reactor systems.

In the following, the bubble wake structure in a liquid-solid suspension[10] is introduced, followed by experimental evidence highlighting the important role of the bubble wake in process systems.

◧ ***Bubble Wake Structure*** • Figure 8a shows a photograph of a relatively large two-dimensional nitrogen bubble rising through a water-774 μm glass bead fluidized bed at Re_b ($=bU_b/\nu$, based on bubble breadth, b) of 8150. The schematic diagram shown in Figure 8b indicates two regions: the primary wake region includes two vortices—on the right-hand side is well-established circulatory motion, and on the left-hand side the vortex is just forming. Outside the primary wake region, there exists a slightly deformed, large vortex that is isolated by streams of external flow across the wake from right to left. As seen in the figure, the solids concentra-

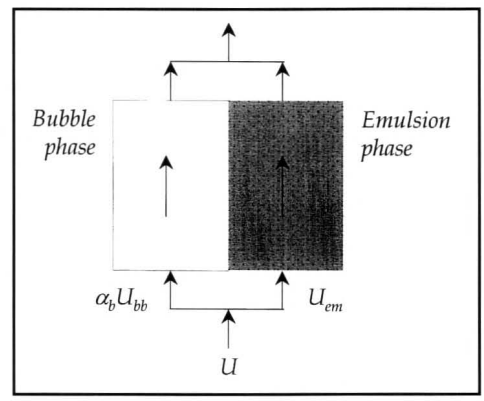

Figure 7. *Gas flow distribution in the bed based on the two-phase theory.*

tion varies within the wake; lower solids concentration regions were observed immediately beneath the bubble base and around the vortex center, while higher concentration regions occurred around the vortices and especially in the regions where the two vortices interact.

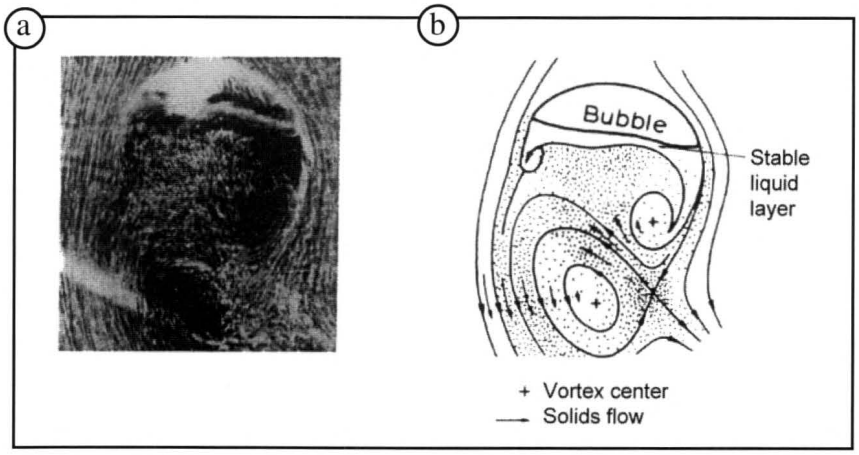

Figure 8. *Bubble wake phenomena in a liquid-solid fluidized bed (from Tsuchiya and Fan;[11] reproduced with permission).*
a) *Photograph of a circular-cap bubble and its wake in a water-774 μm glass bead fluidized bed.*
b) *Schematic interpretation of the wake flow.*

◧ *Bed Contraction* • When gas is introduced to a liquid-solid fluidized bed of small particles (see Figure 9a), contraction instead of expansion of the bed occurs (Figure 9b). An increasing gas flow rate causes further contraction up to a critical gas-flow rate beyond which the bed expands (Figure 9c).[12] Considerable research has been conducted to study the unique bed-expansion characteristics in three-phase fluidization and showed that bed contraction can be attributed to the behavior of the bubble wake. Phenomenologically, bed-contraction phenomena could be explained by the presence of a solids-containing wake, which allows some liquid flow to bypass the liquid-solid fluidized region at a higher velocity. This bypass of liquid reduces the liquid velocity in the liquid-solid fluidized region, thus contributing to the bed contraction. Further increase in the gas velocity increases the gas holdup (or gas volume fraction) in the bed, leading to the bed expansion.

◧ *Bubble Coalescence* • An important clue to the mechanism of bubble coalescence can be obtained through observation of rise patterns of successive bubbles. Figure 10 presents photographs representing the bubble-rise paths observed in two-dimensional water-fluidized bed of 460-μm glass beads (Figure 10a) and 1.5-mm acetate particles (Figure 10b) at a given bubble formation frequency f_b. As shown in the figure, the alternate shedding of the bubble wake yields a series of vortices that establish a staggered, snake-like liquid flow pattern downstream relative to the bubble; the central regions of the shed vortices appear as bright spots. The staggered liquid stream emanating from the leading bubble enhances the zigzag motion of the trailing bubble regardless of particle properties.

The figure demonstrates a bubble-pairing process for two different conditions. In Figure 10a, three bubbles initially rise with equal bubble spacing. As time elapses, the first and second bubbles are paired, with the second bubble being profoundly elongated. These two bubbles eventually collide.

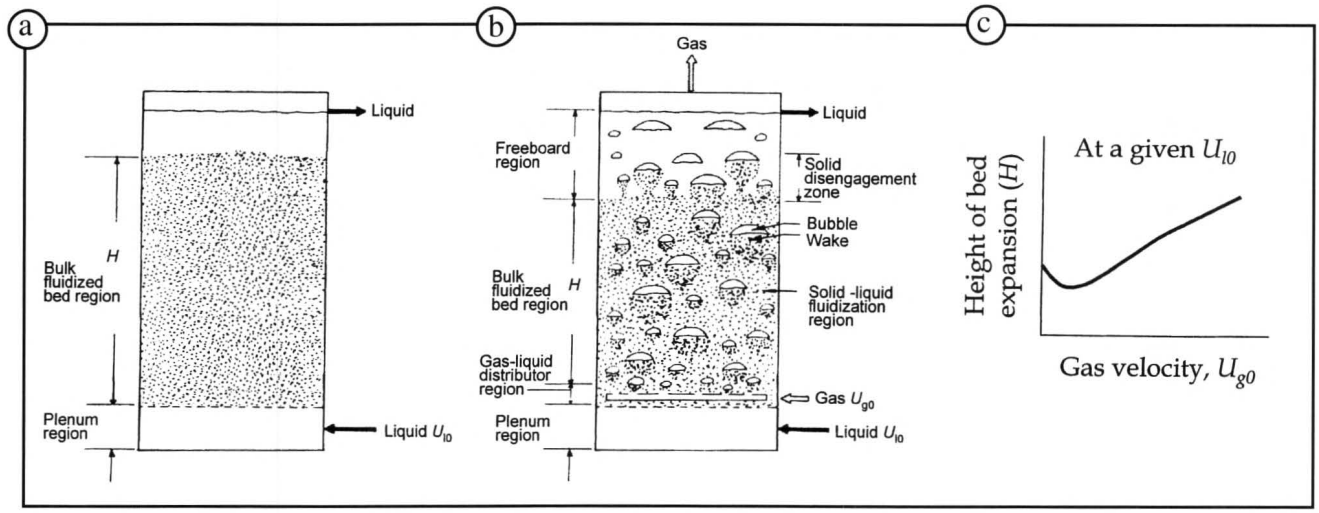

Figure 9. *Bed contraction phenomena in gas-liquid-solid fluidization.*
a) Liquid-solid fluidized bed at U_{l0}.
b) Gas-liquid-solid fluidized bed at U_{l0} and small U_{g0}.
c) Variation of height of bed expansion with gas velocity in a gas-liquid-solid fluidized bed.

A typical "catching up" process is shown in Figure 10b and demonstrates the acceleration of the trailing bubble toward a leading bubble due to the presence of the wake of the leading bubble, which results in bubble pairing and the eventual collision of the pair.

◧ *Particle Entrainment* • The primary wake of a rising bubble and the resulting drift of particles above the upper free surface of a two-dimensional liquid-solid fluidized bed of calcium alginate particles are observed as shown in Figure 11 (next page) (inverse funnel shape). In the photograph, the extent (effective height) of particle carryover through the drift appears to be as significant as that via the bubble wake. The particles carried above the surface are discharged from the wake via wake shedding and are then settled down along with the drift particles as a result of gravitational force. As the freeboard region of a three-phase fluidized bed is based primarily on the particle disengagement behavior from the bubble wake, understanding the wake-shedding behavior allows an accurate design of the freeboard region of a three-phase fluidized bed.

◧ *Precipitation of Calcium Carbonate* • Figure 12 (next page) shows a CO_2 bubble and its wake after injection of 100 bubbles. It is observed that at the early stage of carbonation, the bubble wake is clearly visible as a smoky region, revealing the formation of fine $CaCO_3$ particles. The smoky region is observed in the primary wake, which rises at the same speed as the rising bubble. More fine particles are produced in the wake region than in the bulk region. After injecting 100 bubbles, large "fluffy" aggregates are formed in the bulk region, and the wake region can be distinguished from the particle or aggregate size behind the bubble, as can be seen in the figure. The fluffy aggregates are of loosely packed particles that are easily broken down into smaller fragments by the vortical motion in the bubble wake. Significant changes in the morphology of the fine crystals and in the size distribution of the agglomerates that occur in the wake were observed only during the early stages of the reaction.

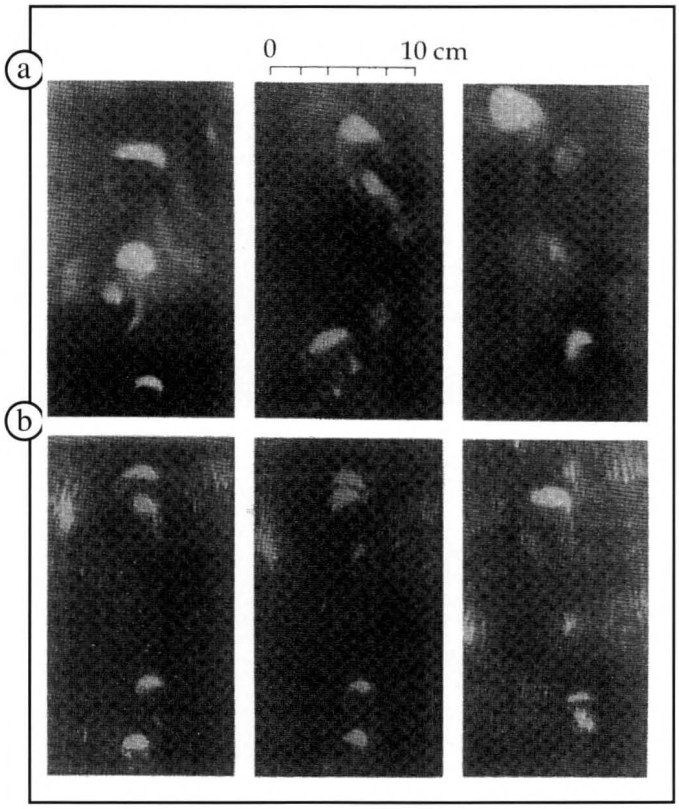

Figure 10. *Bubble pairing followed by bubble collision for successive bubbles in two-dimensional water-solid fluidized beds (from Tsuchiya, et al.;[13] reproduced with permission).*

a) *GB460: b=2.8 cm; f_b=3.1 s^{-1}; Re_b=9180*

b) *AT1500: b=2.0 cm; f_b=3.0 s^{-1}; Re_b=4040*

◧ *Gas-Liquid Mass Transfer* • The mass transfer of gas bubbles is strongly influenced by the bubble- and wake-flow behavior. The solute is carried by the flow on the roof of the bubble along the boundary of the wake and is separated into two regions—within the primary wake region by the wake vortex and outside the wake region by the shedding vortex. The solute that flows into the wake is carried back to the bubble base. The shed vortex carrying the solute generates an external concentration vortex and eventually diffuses into the bulk flow. In addition to the convective diffusion by the liquid-solid flow, there is slow molecular diffusion of solute from the vortex sheet into the vortex center in the wake and from the wake surface into the bulk flow, but these contributions are negligible compared to convective diffusion.

The variations of the mass transfer patterns around bubbles with respect to time are given in Figure 13 (next page). It shows the circular-cap ozone-oxygen bubble and its wake rising in a starch-iodine-water, 0.46-mm glass-bead fluidized bed. As the bubble begins to rise, the reacted ozone molecules are carried from the edge of the bubble by the vortex sheet, and the wake underneath the circular-cap bubble is gradually saturated with ozone molecules. It can be seen that the shape of the bubble plus the wake is approximately circular. The zigzag trail behind the bubble is formed in the bulk of the liquid phase as a result of the vortex shedding. It is interesting to note that there is no trace of ozone molecules on the surface of the bubble roof since the reacted molecules are swept by the liquid flow. As a consequence, the convective diffusion induced by potential flow plays an important role in the mass-transfer mechanism on the bubble roof. As the bubble rises further, the wake (filled completely with gas molecules) starts to shed vortices. As shown in the figure, alternate sheddings are observed in low bed expansion conditions of the liquid-solid fluidized media. The shed vortices elongate their shape and the gas molecules begin to diffuse out from the center of the vortices into the bulk liquid by molecular diffusion, especially in the case of high bed expansion.

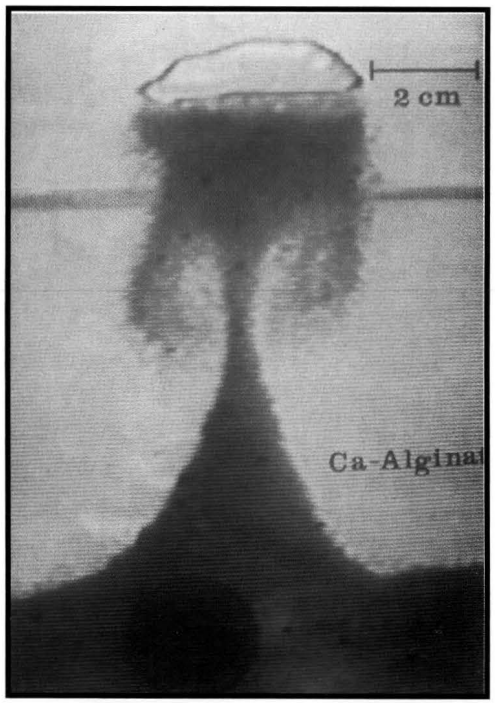

◀ ***Figure 11.***

Entrainment of particles by bubble wake and drift induced by a rising bubble (from Tsuchiya, et al.[14] reproduced with permission of the American Institute of Chemical Engineers, © 1992 AIChE).

Figure 12. ▶

Precipitation of $CaCO_3$ particles from a rising CO_2 bubble (from Tsutsumi, et al.,[15] reproduced with permission).

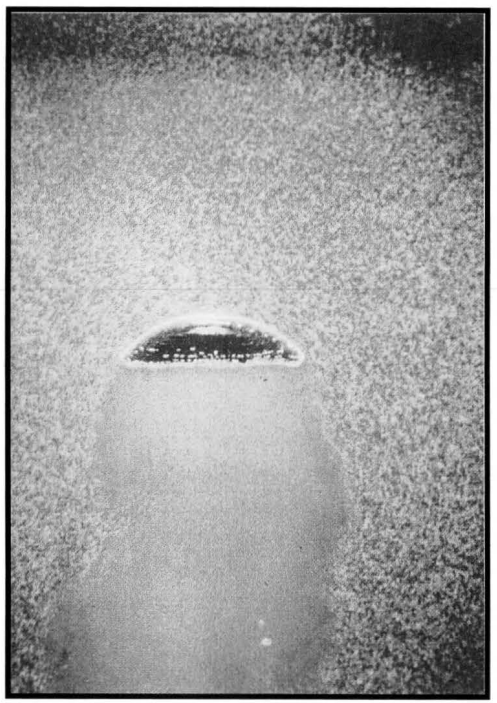

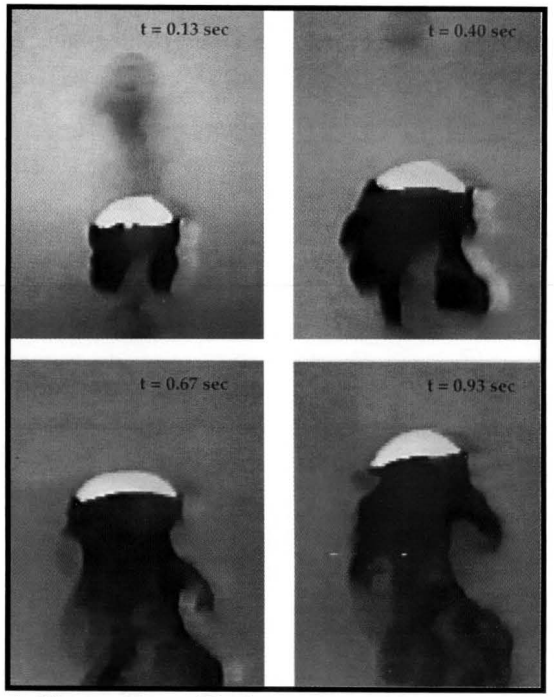

▲ ***Figure 13.***

O_3 bubble rising in a KI-starch solution and 0.46-mm glass-bead fluidized bed.

▼ ***Figure 15.***

Simulation results of bubble formation in a gas-solid fluidized bed using Fluent.

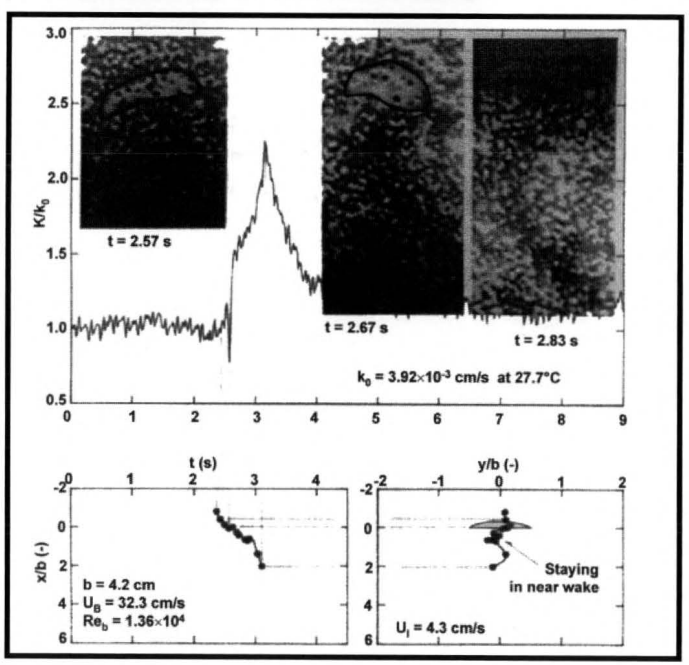

◀ ***Figure 14.***

Instantaneous local liquid-solid mass transfer coefficients in the wake region and the effects of vortices on the primary wake (from Arters, et al.,[16] reproduced with permission).

x - vertical downward distance from the bubble base

y - horizontal right-hand distance from the center of the bubble base

b - bubble breadth

U_B - absolute bubble rise velocity

Re_b - bubble Reynolds number based on the bubble breadth

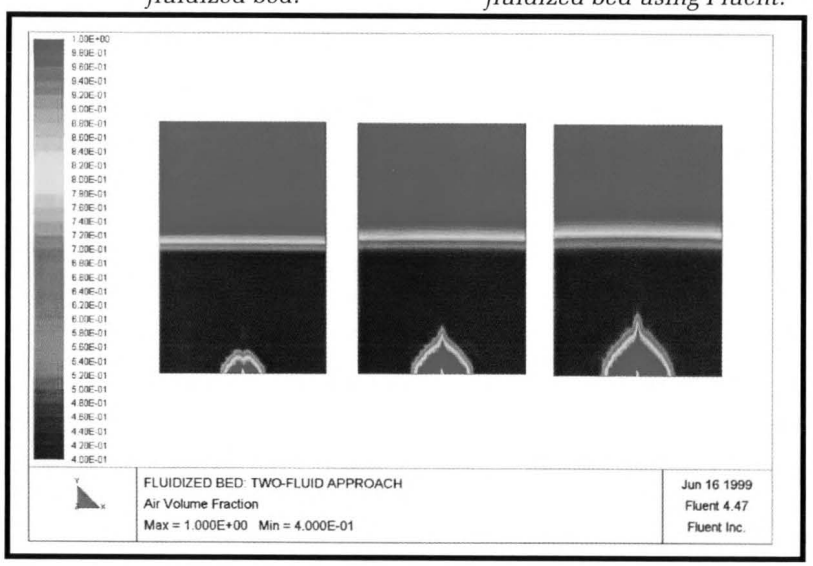

Liquid-Solid Mass Transfer • Mass transfer from the liquid to the surface of the solid, and hence the reaction rate, are governed, apart from the activity of the solid, by the local flow patterns of the liquid relative to the solid. Due to the unique flow structures associated with the liquid in the wake and the presence of solid particles in this region, it is of interest to examine the interaction between a solid particle and a bubble wake and its effect on liquid-solid mass transfer. The instantaneous value of the mass transfer coefficient, k, for a single particle in a two-dimensional liquid-solid fluidized bed, subjected to the disturbance of a single rising gas bubble, can be measured by an electrochemical method using tethered particles. The method measures the limiting current and thereby allows evaluation of k. Visualization techniques can be employed to track the particle in relation to the bubble and bubble wake. Synchronization of the mass-transfer data acquisition with the video record allows a history of the local mass transfer to be analyzed.[16]

Figure 14 shows the liquid-solid mass-transfer behavior interactions of a particle with the bubble and the primary wake. The axes in the figures are linked such that information regarding the mass transfer coefficient, event time, and particle position with respect to dimensionless bubble coordinates can be cross-referenced. The mass transfer coefficient is expressed in terms of k/k_0, where k_0 is the liquid-solid mass transfer coefficient under liquid-solid fluidization conditions at the same liquid velocity. The most salient feature is that the interaction of the particle with the wake region produces substantial increases in the mass transfer coefficient. It can be seen in the figure that a twofold increase in mass transfer results when a particle traveling directly underneath and along with the bubble is ejected from the primary wake through the cross flow. The free shear layer formed at the bubble edge is also found to produce significant increases in mass transfer. Lesser increases are seen when the particle is exposed to a shear layer not strong enough to pull the particle into the flow.

COMPUTATIONAL FLUID DYNAMICS OF PARTICULATE SYSTEMS

Computation is an area of great importance. Students should be kept abreast of the current approach in computation for particulate systems. In the following, a general background on the basic methods of particulate flow computation is introduced and is followed by an example of a state-of-the-art computational problem that my research group is tackling.

General Background • The computational fluid dynamics approach has provided considerable insight into the dynamic behavior of multiphase systems. The Euler-Euler,[17] Euler-Lagrange,[18] and direct[19] numerical simulations are three widely used approaches for particulate-system computation. In the Euler-Euler method, the individual phases are treated as pseudo-continuous fluids, each being governed by the conservation laws expressed in terms of volume/time or ensemble-averaged properties. The conservation equations are closed by constitutive relations that could be obtained from empirical relationships, or theories. The dynamic motion of solid particles, especially for collision-dominated shear flows of solid particles, is often simulated using kinetic theory[20] in which theoretical analogies between the gas molecule and solid particles are applied. In the Lagrangian approach, the discrete particles are treated as a group of point masses with their position, velocity, and other quantities being tracked based on the motion equation of individual particles. The dispersed phase can exchange momentum, mass, and energy with the fluid phase. In the dispersed phase, particle-particle collision dynamics characterize the particle-particle interactions. In direct numerical simulation, the fluid flow could be solved by using finite difference/volume/element discretization of the Navier-Stokes equations, or the lattice-Boltzmann, or Lagrangian multiplier method. Direct numerical simulations require no empirical constitutive equations and could provide detailed information about flow surrounding individual particles.

The Euler-Euler and Euler-Lagrange approaches have been incorporated in many commercial software packages. Fluent (by Fluent, Inc.), CFX (by AEA Technology), Flow3D (by Flow Science, Inc.), and CFDLIB (by Los Alamos National Lab) are some of the common packages used in academia and industry for chemical process applications. The results for a simulation of the bubble formation process in a gas-solid fluidized bed using Fluent 4.47 are shown in Figure 15. In this example, the Euler-Euler two-fluid approach is used to solve the gas and solid flow in a fluidized bed. The rectangular domain is 0.4 m wide by 0.6 m high and is filled halfway with a fluidized bed. The particle diameter used is 0.5 mm with a density of 2610 kg/m^3. Air is used as the gas phase, which has a density of 2.3 kg/m^3 and a viscosity of 1.7 x 10^{-5} kg/m-s. Initially, the bed has a uniform vertical air flow of 0.284 m/s introduced from the lower boundary. When a simulation is started, a vertical air jet is injected from the lower center of the fludized bed. The orifice width of the air jet is 0.03 m. The bubble size is seen to increase significantly with time. Similar results were presented earlier by Sinclair[21] using Fluent 4.32.

Examples of State-Of-The-Art Computation • My research group has been engaged in computation code development for simulation of the gas-liquid-solid fluidization systems.[22] The discrete-phase approach is employed with the volume-averaged method, the discrete-particle method (DPM), and the volume-of-fluid method (VOF) used to account for the flow of liquid, solid, and gas phases, respectively. A bubble-induced force model (BIF), a continuum surface force model (CSF), and Newton's third law are applied to account for the couplings of particle-bubble (gas), gas-liquid, and particle-liquid interactions, respectively. A

close-distance interaction model (CDI) is included in the particle-particle collision analysis, which considers the liquid interstitial effects between colliding particles. The following presents representative results for a single bubble rising and particle entrainment by a single bubble in a liquid-solid fluidized bed under ambient conditions and multi-bubbles rising in a liquid-solid fluidized bed under high-pressure conditions.

The behavior of a single bubble rising in a liquid-solid fluidized bed suspension under ambient conditions is simulated in Figure 16. One thousand particles with a density of 2,500 kg/m^3 and a diameter of 1.0 mm are used as the solid phase. An aqueous glycerin solution (80 wt%) is used as the liquid phase. The superficial liquid velocity is 5 mm/s, yielding a solids holdup of 0.44. It can be seen that the bubble is of spherical-cap shape rising rectilinearly. Also shown in the figure are photographs of a single bubble rising in a liquid-solid fluidized bed obtained experimentally under the same operating conditions as those of the simulation. As shown in the figure, the simulated and experimental results of the bubble-rise velocity and the bubble shape generally agree.

Figure 17 shows the simulated results of particle entrainment by a bubble from the bed

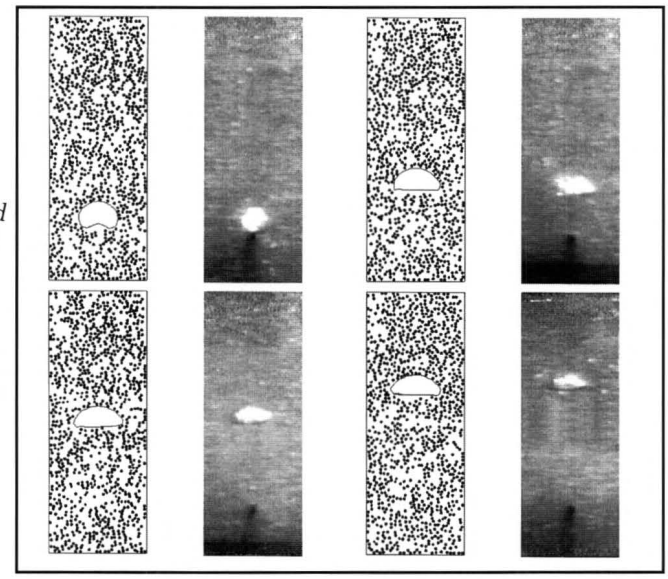

Figure 16. *Simulation and experimental results of a single bubble rising in a liquid-solid fluidized bed.*

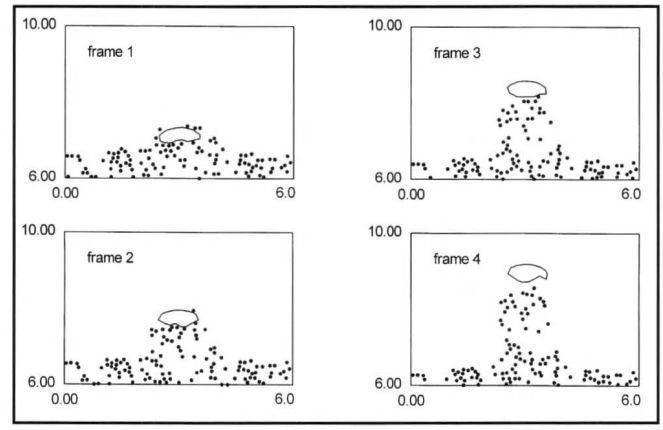

Figure 17. *Simulation results of a bubble emerging from the surface of a liquid-solid fluidized bed.*

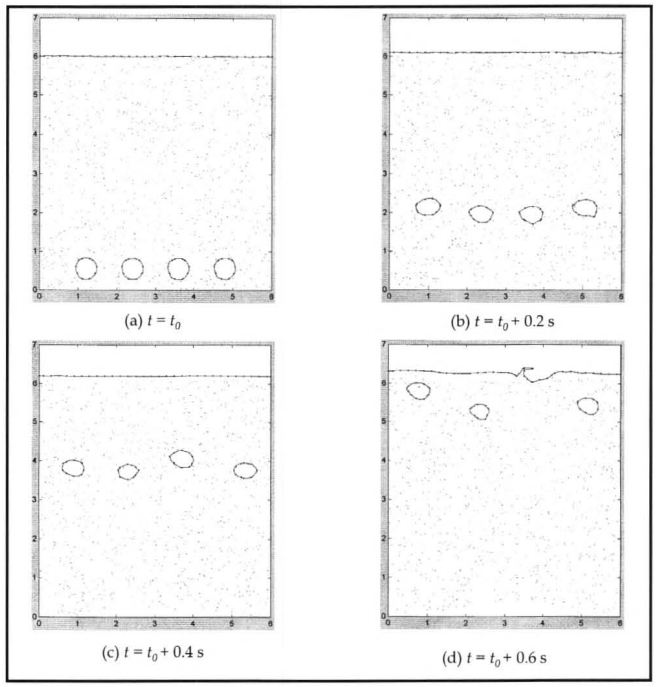

Figure 18. *Simulation results of multi-bubble rising in a liquid-solid fluidized bed at a pressure of 17.3 MPa (ε_s=0.17; d_p=0.5 mm; ρ_p=1,500 kg/m^3; d_b=4.0mm).*

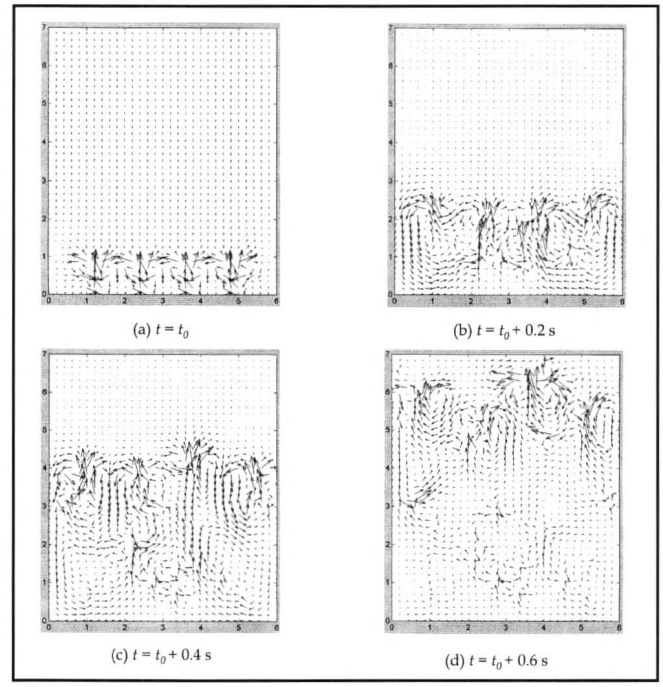

Figure 19. *Simulated velocity vector fields of fluids for the conditions given in Figure 18.*

surface. As seen in the figure, particles are drawn from the upper surface of the suspension into the freeboard of the bed through the wake behind the bubble; and particle-containing vortices are shed from the wake in the freeboard, consistent with the experimental observation shown in Figure 11. Figure 18 shows the rising of four bubbles in a liquid-solid fluidized bed with a solids holdup ε_s of 0.17 and a pressure of 17.3 MPa. The corresponding velocity vector fields of fluids are shown in Figure 19. As can be seen from the figure, the four bubbles are not rising at the same velocity even though their initial conditions are the same. Clearly, complex interactions among gas bubbles, liquid, and solid particles result in nonuniformity of the flow field shown in Figure 19, yielding uneven rise characteristics of the bubbles.

CONCLUDING REMARKS

I would like to conclude my lecture with the following thoughts:

- *Multiphase fluidization is a subject of importance to chemical engineering education as it encompasses the fundamental physics that govern multiphase fluid and particle mechanics and their interactions. Furthermore, interest in the subject is heightened because of its significant industrial applications.*
- *For gas-solid fluidization, topics of most relevance include, for low-velocity fluidization, particle and bubble dynamics, bed stability, bubble-phase and emulsion-phase interaction, and two-phase theory. For high-velocity gas-solid fluidization, the core topics are particle segregation and clustering. For gas-liquid-solid fluidization, the bubble-wake dynamics is key to the fundamental characterization of transport phenomena. In gas-solid or gas-liquid-solid fluidization, the particle property, which is an important operating variable, affects the fluidization regimes and their transitions.*
- *The computational fluid dynamics approach has provided a viable means for flow system and chemical reactor characterization. Although available commercial codes may not always yield accurate predictions, the familiarity of students with these computational tools would fortify their capability of understanding complex multiphase fluidization systems.*

ACKNOWLEDGMENTS

This lecture is dedicated to the memory of Professor Shao-Lee Soo of the University of Illinois, Urbana. I benefited from Prof. John Davidson's lecture on fluidization seven years ago when I was on sabbatical at Cambridge University, in which he demonstrated the simple slug-rising device that I duplicated, shown in Figure 2. I am indebted to Prof. Jack Zakin and my research group members, Dr. Jianping Zhang, Mr. D.-J. Lee, Mr. Brian McLain, Mr. Will Peng, and Mr. Guoqiang Yang, who have provided constructive feedback in the preparation of this lecture material.

REFERENCES

1. Geldart, D., "Types of Gas Fluidization," *Powder Tech.,* **7**, 285 (1973)
2. Anderson, T.B., and R. Jackson, "A Fluid Mechanical Description of Fluidized Beds: Stability of the State of Uniform Fluidization," *I&EC Fund.,* **7**, 12 (1968)
3. Kunii, D., and O. Levenspiel, *Fluidization Engineering,* 2nd ed., Butterworth-Heinemann, Boston, MA (1991)
4. Rowe, P.N., "Experimental Properties of Bubbles," in *Fluidization,* J.F. Davison and D. Harrison, eds., Academic Press, New York, NY (1971)
5. Davison, J.F., and D. Harrison, *Fluidized Particles,* Cambridge University Press, Cambridge, UK (1963)
6. Reuter, H., "Druckverteilung um Blasen im Gas-Feststoff-Fließbett," *Chem-Ing.-Tech.,* **35**, 98 (1963)
7. Reuter, H., "Mechanismus der Blasen im Gas-Feststoff-Fließbett," *Chem-Ing.-Tech.,* **35**, 219 (1963)
8. Stewart, P.S.B., "Isolated Bubbles in Fluidized Beds: Theory and Experiments," *Trans. Instn. Chem. Engrs.,* **46**, T60(1968)
9. Toomey, R.D., and H.F. Johnstone, "Gaseous Fluidization of Solid Particles," *Chem. Eng. Prog.,* **48**, 220 (1952)
10. Fan, L.-S., and K. Tsuchiya, *Bubble Wake Dynamics in Liquids and Liquid-Solid Suspensions,* Butterworth-Heinemann, Boston, MA (1990)
11. Tsuchiya, K., and L.-S. Fan, "Near-Wake Structure of a Single Gas Bubble in a Two-Dimensional Liquid-Solid Fluidized Bed: Vortex Shedding and Wake Size Variation," *Chem. Eng. Sci.,* **43**, 1167 (1988)
12. Massimilla, L., N. Majuri, and P. Signorini, "Sull'assorbimento di Gas in Sistema: Solido-Liquido, Fluidizzato," *La Ricerca Scientifica,* **29**, 1934 (1959)
13. Tsuchiya, K., T. Miyahara, and L.-S. Fan, "Visualization of Bubble-Wake Interactions for a Stream of Bubbles in a Two-Dimensional Liquid-Solid Fluidized Bed," *Int. J. Multiphase Flow,* **15**, 35 (1989)
14. Tsuchiya, K., G.-H. Song, W.-T. Tang, and L.-S. Fan, "Particle Drift Induced by a Bubble in a Liquid-Solid Fluidized Bed with Low-Density Particles," *AIChE J.,* **38**, 1847 (1992)
15. Tsutsumi, A., J.-Y. Nieh, and L.-S. Fan, "Role of the Bubble Wake in Fine Particle Production of Calcium Carbonate in Bubble Column Systems," *I&EC Res.,* **30**, 2328 (1991)
16. Arters, D.C., K. Tsuchiya, and L.-S. Fan, "Solid-Liquid Mass Transfer in the Wake Region Behind a Single Bubble in a Liquid-Solid Fluidized Bed," in *Fluidization VI,* J.R. Grace, L.W. Shemilt, and M.A. Bergougnou, eds., Engineering Foundation, pp. 507-514 (1989)
17. Sinclair, J.L., and R. Jackson, "Gas-Particle Flow in a Vertical Pipe with Particle-Particle Interactions," *AIChE J.,* **35**, 1473 (1989)
18. Hoomans, B.P.B., J.A.M. Kuipers, W.J. Briels, and W.P.M. van Swaaij, "Discrete Particle Simulation of Bubble and Slug Formation in a Two-Dimensional Gas-Fluidized Bed: A Hard Sphere Approach," *Chem. Eng. Sci.,* **51**, 99 (1996)
19. Joseph, D.D., "Interrogation of Numerical Simulation for Modeling of Flow Induced Microstructure," *ASME FED,* **189**, 31 (1994)
20. Jenkins, J.T., and S.B. Savage, "A Theory for the Rapid Flow of Identical, Smooth, Nearly Elastic, Spherical Particles," *J. Fluid Mech.,* **130**, 187 (1983)
21. Sinclair, J.L., "CFD Case Studies in Fluid-Particle Flow," *Chem. Eng. Ed.,* **31**, 108 (1998)
22. Li, Y., J. Zhang, and L.-S. Fan, "Numerical Simulation of Gas-Liquid-Solid Fluidization Systems Using a Combined CFD-DPM-VOF Method: Bubble Wake Behavior," *Chem. Eng. Sci.,* **54**, 5101 (1999) ❐